Philosophical Magazine

ISSN: 1478-6435 (Print) 1478-6443 (Online) Journal homepage: http://www.tandfonline.com/loi/tphm20

First principle study of structural, elastic and electronic properties of APt_3 (A=Mg, Sc, Y and Zr)

A. Benamer, A. Roumili, Y. Medkour & Z. Charifi

To cite this article: A. Benamer, A. Roumili, Y. Medkour & Z. Charifi (2017): First principle study of structural, elastic and electronic properties of APt_3 (A=Mg, Sc, Y and Zr), Philosophical Magazine, DOI: 10.1080/14786435.2017.1407879

To link to this article: https://doi.org/10.1080/14786435.2017.1407879

Published online: 27 Nov 2017.

PHILOSOPHICAL MAGAZINE, 2017
https://doi.org/10.1080/14786435.2017.1407879

Taylor & Francis
Taylor & Francis Group

First principle study of structural, elastic and electronic properties of APt_3 (A=Mg, Sc, Y and Zr)

A. Benamer[a], A. Roumili[a], Y. Medkour[a] and Z. Charifi[b,c]

[a]Laboratoire d'Etudes des Surfaces et Interfaces des Matériaux Solides (LESIMS), Université de Setif1, Setif, Algeria; [b]Department of Physics, Faculty of Science, University of M'sila, M'sila, Algeria; [c]Laboratory of Physics and Chemistry of Materials, University of M'sila, M'sila, Algeria

ABSTRACT

We report results obtained from first principle calculations on APt_3 compounds with A=Mg, Sc, Y and Zr. Our results of the lattice parameter a are in good agreement with experimental data, with deviations less than 0.8%. Single crystal elastic constants are calculated, then polycrystalline elastic moduli (bulk, shear and Young moduli, Poisson ration, anisotropy factor) are presented. Based on Debye model, Debye temperature Θ_D is calculated from the sound velocities V_l, V_t and V_m. Band structure results show that the studied compounds are electrical conductors, the conduction mechanism is assured by Pt-d electrons. Different hybridisation states are observed between Pt-d and A-d orbitals. The study of the charge density distribution and the population analysis shows the coexistence of ionic, covalent and metallic bonds.

ARTICLE HISTORY
Received 30 April 2017
Accepted 14 November 2017

KEYWORDS
Intermetallic compounds; *Ab initio* calculations; elastic properties; electronic structure; thermodynamic

1. Introduction

Intermetallic compounds have shown attractive and unusual properties such as high melting point [1], superconductivity [2], magnetic properties [3,4], corrosion resistance [5], that's made them important materials for various applications field. These binary compounds have the general formula AB_3 where A=Mg, Sc, Y, Zr, Nb, Lu, while B=Ru, Rh, Pd and Pt [2,6]. The unit cell of these compounds is cubic with A elements at 1a (0, 0, 0), B elements at 3c (1/2, 1/2, 0) [2]. Structural, magnetic and electrical properties of YPd_3 was studied by Pandey et al. [3], they succeed to prepare an ultra pure YPd_3 that expected to exhibit a pure diamagnetic character at lower magnetic fields. Using linear-muffin-tin-orbital (LMTO) method, the optical conductivity of APd_3 (A=Sc, Y, La and Ce) was studied and the optical transitions were discussed [7]. Theoretical calculations of electronic structure and magnetic properties of $ScPd_3$ show that this compound has a stable non magnetic

CONTACT Z. Charifi charifizoulikha@gmail.com

state. Furthermore, *d* electrons of Sc and Pd atoms play dominant role near the Fermi level [8]. Pt-based alloys are generally used for high temperature application because of their high melting point [5,6,9–13]. The structural, elastic, electronic and phonon properties of ScX_3 (X = Ir, Pd, Pt and Rh) and APt_3 (A=Sc, Y) have been investigated using density functional theory [12–14], the results show that these compounds exhibit metallic character. Moreover, both of $ScPt_3$ and $ScPd_3$ alloys could be used as materials for ultra high temperature applications.

To complete the earlier works on $ScPt_3$ and YPt_3, we report in this paper a detail study of the structural, elastic, thermal and electronic properties of $MgPt_3$, $ScPt_3$, YPt_3 and $ZrPt_3$. Thereafter, we present the computational details in Section 2. In Section 3, various results were presented and discussed, such as lattice parameters, single crystal elastic constant C_{ij}, polycrystalline elastic moduli, temperature and pressure effects on various structural and fundamental physical parameters, electronic properties and chemical bonding. This work was finished by a conclusion of the main results in Section 4.

2. Calculation details

CASTEP (Cambridge Serial Total Energy Package) code [15] was used to perform this study. The problem of fundamental eigenvalue is resolved using the density functional theory [16] and the Kohn–Sham approach [17]. In the purpose of reducing the very important number of plane waves (PW), that's describe the electron functions, a fictive potential (pseudopotential) is generated to replace the real atomic potential [18]. Pseudo atomic calculations were performed with; Mg: $2p^6 3s^2$, Sc: $3s^2 3p^6 3d^1 4s^2$, Y: $4d^1 5s^2$, Zr: $4s^2 4p^6 4d^2 5s^2$ and Pt: $5d^9 6s^1$. Local density approximation LDA with the CA-PZ functional [19] was used to calculate the exchange correlation energy. The Broyden– Fletcher–Goldfarb–Shanno (BFGS) algorithm [20,21] was used to find the fundamental energy of the crystal. After careful convergence tests, we have used 120 irreducible *k* points to sample the first Brillouin zone [22]. The ultra-soft pseudopotential was employed [21] with a cut-off energy $E_{\text{cut off}} = 500$ eV. Calculations were done since the energy tolerance is about 5.10^{-6} eV/atom, the maximum force is equal to 0.01 eV/ Å, the maximum stress is lower than 0.02 GPa and a maximum displacement doesn't exceed 5.10^{-4}Å.

For elastic constants calculations, the used convergence parameters are; the energy change between two successive cycles is less than 10^{-6} eV/atom, maximum force within 0.002 eV/Å and maximum displacement less than 10^{-4}Å.

3. Results and discussions

3.1. Structural properties

The structure of APt_3 compounds belongs to the $AuCu_3$ type structure [2], A atoms occupy the corners, while Pt atoms set on the face centres. The present results of

the lattice parameter are in good agreement with the available experimental data [2], the deviation between calculated equilibrium volumes and the corresponding experimental ones is less than 2.4%. Calculated equilibrium volumes are in correlation with the atomic radii of A atoms, crossing down the periodic Table increases the equilibrium volume by about 8%. However, increasing the atomic number in the same line reduces the equilibrium volumes by about 4.4%. We note that the Pt atoms are the same in the four compounds, the size of X atoms is different.The different size of the A atoms could be responsible for the lattice constant increasing from MgPt to YPt.The negative values of the calculated cohesive energy [23] reflect the stability of these compounds. It is noted that the APt_3 compounds are more stable when the A element is a transition metal. *E*–*V* data are fitted to the third Birch–Murnaghan equation of state, and the obtained results of the bulk modulus *B* and its pressure derivative B' are summarised in Table 1. One can observe that $ZrPt_3$ has the highest bulk modulus, while YPt_3 has the lowest one. As a result, it is predicted that $ZrPt_3$ is the hardest in the studied series So we conclude that in these type of materials the electrons d play an important role in the hardness of the material. Our results are about 12 and 25% higher than those reported for $ScPt_3$ and YPt_3, respectively [13], this discrepancy could be explained by the use of LDA in the former and the GGA in the later [23]. $ZrPt_3$ presents the lowest dependency to external pressure. The obtained results for the bulk modulus are in good agreement with the well-known relation the smallest unit cell volume, the highest bulk modulus.

3.2. Elastic constants and their related properties

The study of elastic behaviour of materials is very important for both academic and technological aspect, in the former, elastic constants are related to many microscopic parameters such as chemical bonding, for the later, they are related to macroscopic properties such as fatigue, cracks, dislocations. Results of single crystal elastic constants C_{ij} are carried out based on the finite elastic strain technique [24–26]. Elastic properties of a cubic crystal can be described using three independent

Table 1. Summary of calculated lattice parameters, cohesive energy E_{coh}, bulk modulus *B* and its pressure derivative *B*′.

		a (Å)	*V* (Å)^3	E_{coh} (eV)	*B* (GPa)	*B*′
$MgPt_3$	Our calc.	3.898	59.24	−6.65	235	5.3
	Exp[2]	3.918	60.14			
$ScPt_3$	Our calc.	3.935	60.92	−8.02	253	5.2
	Exp[2]	3.958	62.00			
	Calc.	4.024 [12] 4.003 [13]			208[13]	5.3[13]
YPt3	Our calc.	4.041	65.94	−7.96	219	5.1
	Exp[2]	4.075	67.66			
	Calc.	4.024 [12] 4.081 [13]			175[13]	5.4[13]
$ZrPt_3$	Our calc.	3.980	63.03	−8.76	274	5.0
	Exp[2]	3.990	63.52			

Table 2. Calculated single crystal elastic constants and related polycrystalline elastic moduli.

	Method	$MgPt_3$	$ScPt_3$	YPt_3	$ZrPt_3$
C^{11}	Our cal.	322	371–286 [10]–350 [11]	309	399
C^{44}	Our cal.	134	139–113 [10]–72 [11]	110	144
C^{12}	Our cal.	189	194–154 [10]–194 [11]	174	211
B (GPa)	Our cal.	233	253	219	274
	Other cal.		221 [10] 246 [11]		
G (GPa)	Our cal.	101	116	90	121
	Other cal.	94[10]/74[11]			
G' (GPa)	Our cal.	66.5	88	67	94
	Other cal.		66 [10]/78 [11]		
CP (GPa)	Our cal.	55	55	64	67
E (GPa)	Our cal.	264	301	237	316
	Other cal.		245 [10]/203 [11]		
Hv	Our cal.	8.20	9.95	6.91	9.79
v	Our cal.	0.3106	0.3011	0.3192	0.3075
	Other cal.		0.302 [10]/0.360 [11]		
A^U	Our cal.	2.015	1.5706	1.6296	1.53
	Other cal.				
B/G	Our cal.	2.3	2.18	2.43	2.2644
	Other cal.		2.0 [10]/3.33 [11]		

elastic constants C_{11}, C_{12} and C_{44} [27]. Our results for C_{ij} are summarised in Table 2 with previous calculated data for $ScPt_3$. The requirements for mechanical stability of the cubic system at 0 GPa are [24]: $C_{11}-C_{12} > 0$; $C_{11} + 2C_{12} > 0$ and $C_{44} > 0$, these conditions are well satisfied by the values reported in Table 2. These ensure the mechanical stability of the previously studied compounds. Our results are in good agreement with those reported in [12,14]. C_{11} is related to the unidirectional compression along the principal directions, the highest (lowest) value is that of $ZrPt_3$ (YPt_3).This confirms the results found is Section 3.1 that $ZrPt_3$compound is the hardest one. Shear modulus C_{44} changes from 144 GPa for $ZrPt_3$ to 110 GPa for YPt_3. We have examine the dependency of C_{ij} to external hydrostatic pressure until 50 GPa, according to the mechanical stability criteria [28], these compounds remain stable up to 50 GPa and no phase transition is expected. Single crystal elastic constants increase linearly with increasing pressure. C_{11} has the most dependency (dC_{11}/dp) to external pressure, while C_{12} has the lowest dependency (dC_{12}/dp) to pressure. It is clearly seen that, increasing pressure up to 50 GPa, leads to increase C_{11}, C_{44} and C_{12} elastic constants (see Figure 1).

Polycrystalline elastic constants are more meaningful for technological aspects, in this study they are presented using only the Hill's assumption, which is defined as the arithmetic average of the Voigt and Reuss approximations [26]. The bulk modulus *B* gives information about resistance to volume changes. However, shear modulus *G* provides information on shape change resistance [26]. Brittleness and ductility properties of APt_3 (A=Mg, Sc, Y and Zr) compounds have been investigated by calculating the *B*/*G*. The critical value that separates brittleness and ductility is around 1.75. If *B*/*G* value is smaller than 1.75, the material behaves in a brittle manner; otherwise, the material is a ductile compound.

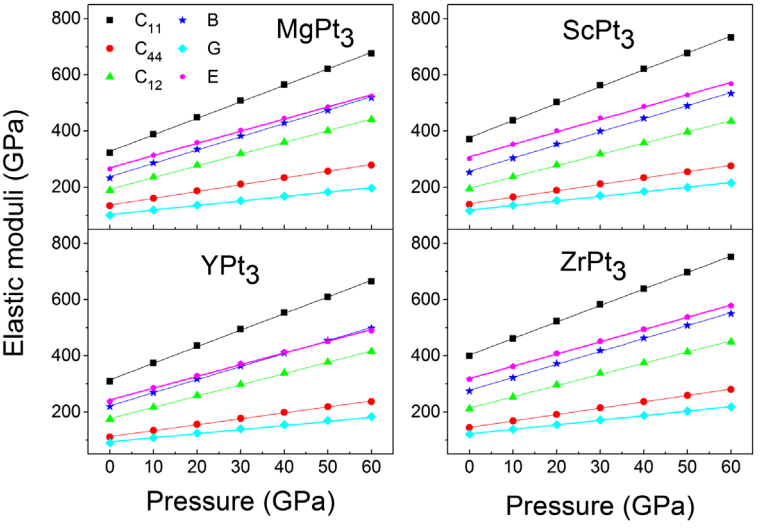

Figure 1. (Colour online) Pressure effect on elastic moduli of APt_3 with A=Mg, Sc, Y and Zr.

Our results for the bulk modulus B, shear modulus G, tetragonal shear modulus $G' = (C_{11}-C_{12})/2$, Young's modulus Y, Poisson's ratio P, anisotropy factor A and Pugh's criterion B/G for the ductility or brittleness are summarised in Table 2.

Firstly, we note the excellent agreement of calculated bulk modulus using the EOS and the C_{ij} of single crytal. Bulk modulus takes values between 219 GPa for YPt_3 and 274 GPa for $ZrPt_3$, the only available study is on $ScPt_3$, the calculated bulk modulus is consistent with the reported one of Razumovski et al. [14], however it is about 10% higher than the reported one by Arikan et al. [12]. According to our results, we observe a decrease of the bulk modulus when going from (Sc → Y), however it increases from (Y → Zr). These results agree with the relation between the lattice parameter and the bulk modulus (B α $1/V$) [29]. The resistance to shape change (G) is about 50% lower than the resistance to volume change (B) of these compounds. The highest resistance to shear deformation (G or G') is that of $ZrPt_3$, moreover, the sequence $B > G > G'$ clearly demonstrates that the tetragonal shear modulus G' presents the lower boundary of the mechanical stability for these compounds. Our results for $ScPt_3$ are higher than those reported in [12,14]. Young's modulus E describes the behaviour of a material versus one directional stress and gives a measure of the stiffness. $ZrPt_3$ presents the higher stiffness, however YPt_3 presents the lower one. The only available data on $ScPt_3$ for the Young modulus, show that our results are respectively 11 and 34% higher than those reported in [12,14], this discrepancy can be explained by the use of LDA which is well-known to underestimates the lattice parameters and overestimates the elastic constants [16]. The pressure effect, up to 50 GPa, on the bulk modulus B, shear modulus G and Young modulus Y is presented in Figure 1. According to our results B and Y increase faster than G with increasing pressure. Thereby, in this family of APt_3,

Table 3. Results of calculated densities, sound velocities, Debye's temperatures and melting temperature.

Compounds	Bonds	Bond length (Å)	Population (\e\)	Charge (\e\)
$MgPt_3$	Pt–Pt	2.75616	0.94	Mg:2.05
	Pt–Mg	2.75616	−1.58	Pt:−0.68
$ScPt_3$	Pt–Pt	2.78284	0.9	Sc: 1.23
	Pt–Sc	2.78284	−0.14	Pt: −0.41
YPt_3	Pt–Pt	2.85748	1.13	Y: 1.55
	Pt–Y	2.85748	−0.63	Pt : −0.52
$ZrPt_3$	Pt–Pt	2.81434	0.76	Zr: 1.11
	Pt–Zr	2.81434	0.07	Pt: −0.37

the resistance to volume changes and the strength increase rapidly with pressure, however the resistance to shape change increases slightly with pressure.

Cauchy's pressure *CP* gives us some information about the type of atomic bonding in the crystal, *CP* is negative (positive) for predominate covalent (metallic) bonding [30], as reported in Table 2, the present compounds have positive *CP* values which is a characteristic of metallic bonding. As reported by Haines et al. [31], 0.25 is a typical value of Poisson's ratio for ionic bonding, values around 0.33 are a signature of metallic bonding. The obtained values are greater than 0.3, and again this suggest the presence of metallic bonds in these compounds.

Elastic anisotropy is related to the highly directional chemical bonding, For isotropic materials $A = 1$, however any deviation of A from unity suggests elastic anisotropy [27]. The calculated anisotropy factors are larger than the unity, and then our compounds are all elastically anisotropic and we can expected the presence of directional bonding in these compounds. The Pugh's factor B/G expresses the malleability of a material. The B/G values higher than 1.75 indicate a ductile behaviour, while the values lower than 1.75 indicate brittleness [32]. According to the values of B/G reported in Table 2, the studied compounds are ductile materials, which is in good agreement with the low resistance to shear deformation.

Based on Debye's model [33], we have calculated the Debye's temperature Θ_D from the longitudinal V_l and the transversal V_t velocities of the elastic waves as shown in Table 3. For $ScPt_3$, our calculated Θ_D is in agreement with the reported one in [12]. Therefore, and according to the relation between the melting temperature (T_m) and Θ_D ($T_m \sim \Theta_D$) [33], we can suggest that $ScPt_3$ and $ZrPt_3$ have the higher melting temperature.

According to this study, elastic constants and their related parameters decrease (increase) when increasing the atomic number in the same column (line) of the periodic table.We should also add the effect of d electrons is of important role on the mechanical properties of materials under study.

3.3. Thermodynamic properties

Pressure and temperature are important factors in developing new functional materials. In order to examine the present compounds against increasing pressure

and temperature we have used the quasi-harmonic Debye model from which many studies were carried out, the calculations details are well explained elsewhere [33–35].

At first, we have studied the pressure dependency of the normalised volume at a given temperature 0, 300 and 1600 K. The obtained results are plotted in Figure 2. For 0 and 300 K, the pressure effect on the unit cell volume is almost identical. However, for high temperature 1600 K, the normalised volume drops down rapidly with increasing pressure. YPt_3 presents the higher contraction (18%), while $ZrPt_3$ presents the lower one (15%). As results, the bulk modulus at high temperature maintains the same sequence, the $ZrPt_3$ possesses the highest bulk modulus and the YPt_3 the lowest one as summarised in Table 1.

Debye temperature Θ_D is an essential parameter in the investigation of physical properties of materials, it can be related to the elastic constants and the melting point temperature of a material [33]. We present the pressure dependence of the Debye temperature at 0, 300 and 1600 K in Figure 3. In Table 4, we summarised the values of Θ_D at pressures 0 and 50 GPa, and at temperatures 0, 300 and 1600 K, the values of Θ_D for $ScPt_3$ and $ZrPt_3$ are very close, YPt_3 has the lowest one. At 0 GPa, the increase of temperature till 1500 K, reduces the Debye's temperature Θ_D by about 15, 12, 14, 10% for $MgPt_3$, $ScPt_3$, YPt_3 and $ZrPt_3$, respectively. In the other side and as shown in Figure 4. At zero pressure Θ_D is almost independent to temperature when the last one is less than 300 K. It can be observed that Θ_D increases rapidly with pressure, $ZrPt_3$ has the lowest dependency rate to pressure, while YPt_3 has the highest one.

Volume thermal expansion α_v increases (decreases) rapidly with temperature (pressure). Independently to external pressure and temperature, $MgPt_3$ ($ZrPt_3$)

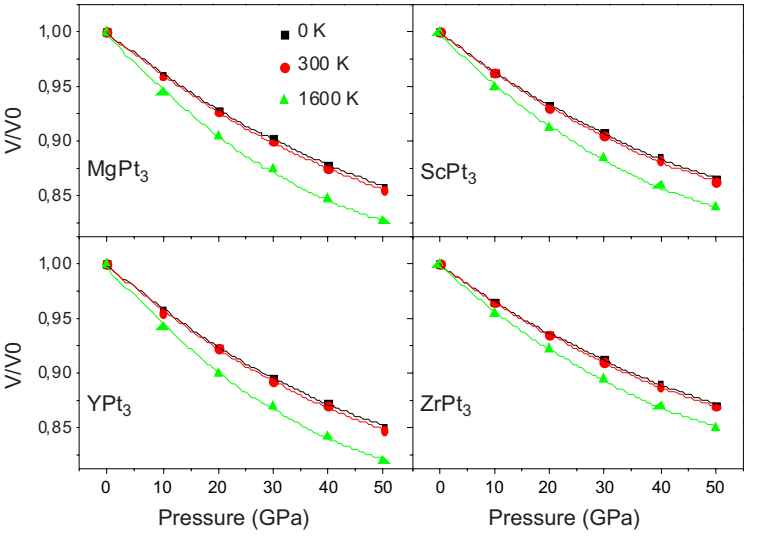

Figure 2. (Colour online) Normalised volume at various temperatures as a function of pressure for APt_3 with A=Mg, Sc, Y and Zr.

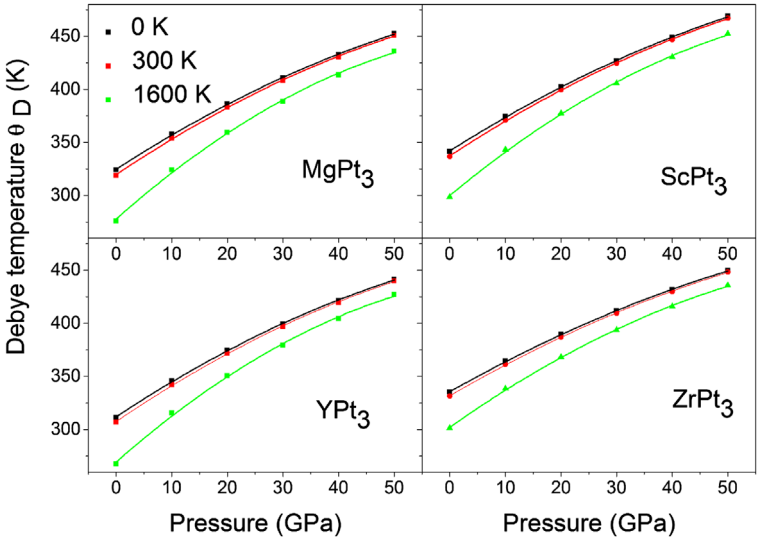

Figure 3. (Colour online) Debye's temperature at various temperatures as a function of pressure for APt_3 with A=Mg, Sc, Y and Zr.

Table 4. Summary of calculated unit cell volume V_{uc}, bulk modulus B, volume thermal expansion α_v, thermal Gruneisen parameter γ_{th}, heat capacities (C_v and C_p) and Debye temperature Θ_D at selected pressures and temperatures.

	Method	$MgPt_3$	$ScPt_3$	YPt_3	$ZrPt_3$
ρ (g cm^{-3})	Our calc.	17.085	17.1768	16.9763	17.8227
V_l (ms^{-1})	Our calc.	4638	4871	4468	4942
V_t (ms^{-1})	Our calc.	2431	2598	2302	2605
V_m (ms^{-1})	Our calc.	2719	2903	2578	2913
Θ_D (K)	Our calc.	330	349	302	346
	Other cal.		398[10]		
$T_m \pm 300$ K	Our calc.	2456	2745	2379	2911

possesses the highest (lowest) volume expansion factors. Thermal Gruneisen parameter γ_{th} that expresses the effect of temperature on vibrational properties of the crystal. At zero pressure and for temperature less than 300 K, the thermal Gruneisen parameter γ_{th} is about 2.5, and increases by about 16, 12, 16 and 8% at 1500 K for $MgPt_3$, $ScPt_3$, YPt_3 and $ZrPt_3$, respectively. However, it decreases by about 25% at pressure of 50 GPa for the considered compounds.

Heat capacity at constant volume C_v of $MgPt_3$, $ScPt_3$, YPt_3 and $ZrPt_3$ as a function of temperature at a given pressure is presented in Figure 4. Firstly, as increasing pressure from 0 to 50 GPa, one can observed that C_v decreases slightly for temperatures less than 300 K. For temperature higher than 500 K, the pressure effect on C_v is insignificant. For all compounds under study and for temperature less than 300 K, the heat capacity C_v increases rapidly with temperature. At higher temperature values C_v increases slowly and reached the classical limit of Dulong-Petit: $C_v = 3\ nR$ [33]. At normal conditions (0 GPa and 300 K), heat capacity at

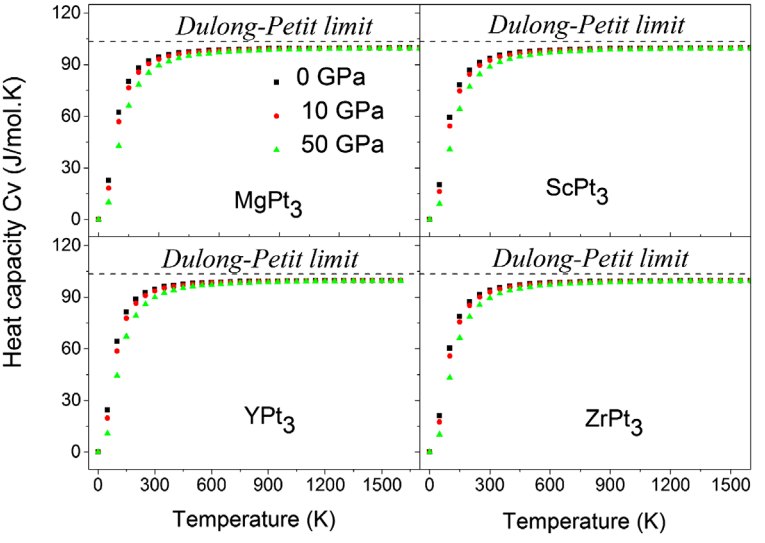

Figure 4. (Colour online) Heat capacity C_v at various pressures as a function of temperature for Apt_3 with A=Mg, Sc, Y and Zr.

constant pressure C_p is about 96.5 (J/mol K) for all compounds. At high temperature C_p increases to 121.7, 117.2, 120.2 and 112.8 (J/mol K) for $MgPt_3$, $ScPt_3$, YPt_3 and $ZrPt_3$, respectively. These values decrease by 14, 12, 13, and 9% at high pressure.

At normal condition of pressure and temperature (0 GPa, 300 K), calculated thermal constants are slightly affected by the substitution of A elements (A=Mg, Sc, Y and Zr).

3.4. Electronic properties and chemical bonding

In order to find out more information about the bonding stiffness from electronic characteristics [36,37], we have calculated the band structure, the density of states, and the charge density distribution. In Figure 5, we present the band structure for the investigated compounds. The energy dispersion spectrum crosses the Fermi level, sets at 0 eV, in the vicinity of R and γ points, then these compounds are conductors. Furthermore, the location of Fermi level close to the minimum of the total density of state suggests a good stability of these compounds [38]. We can also see that this minimum move to lower energies for $ZrPt_3$. This is an indication that this compound is more stable than $MgPt_3$, $ScPt_3$ and YPt_3 compounds.

Based on Figures 6 and 7, the valence band structure of $MgPt_3$ is derived from Pt-d electrons and few Mg–p, Pt-(s,p) states. For the other compounds with A=Sc, Y and Zr, the valence band is derived essentially from Pt-d and A-d electrons and little amount of s and p electrons of Pt and A atoms. At Fermi level, Pt-d electrons are majority except for $ZrPt_3$ where the contribution of Zr-d electrons is higher than Pt-d electrons. The conduction band of $MgPt_3$ is built from Mg-(s,p) and

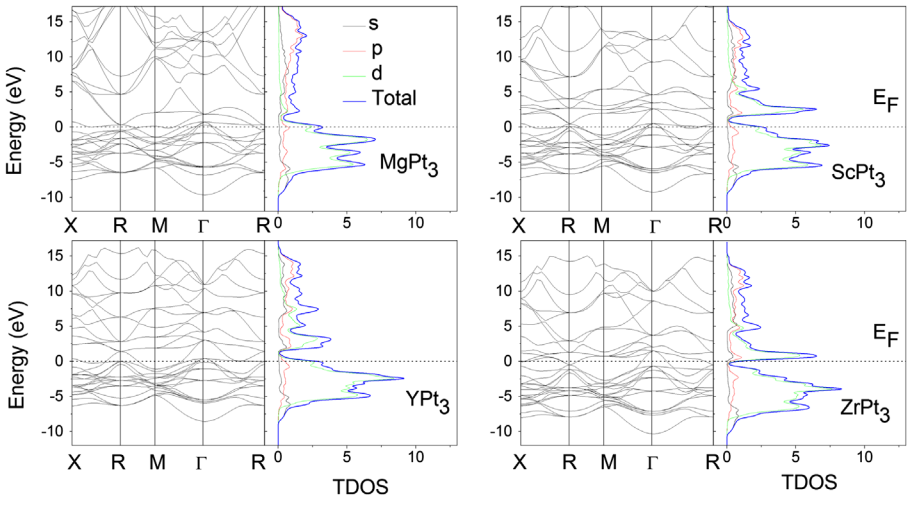

Figure 5. (Colour online) Calculated band structure and total density of states (TDOS) for APt_3 with A=Mg, Sc, Y and Zr.

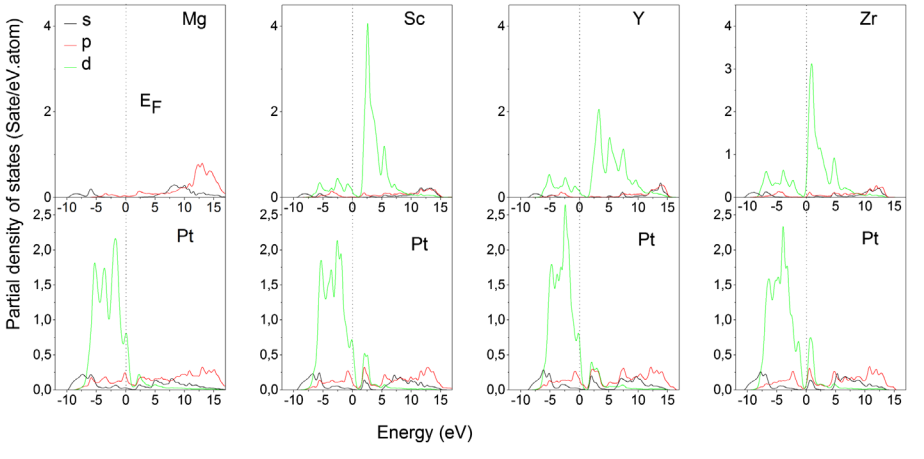

Figure 6. (Colour online) Calculated partial densities of states for APt_3 with A=Mg, Sc, Y and Zr.

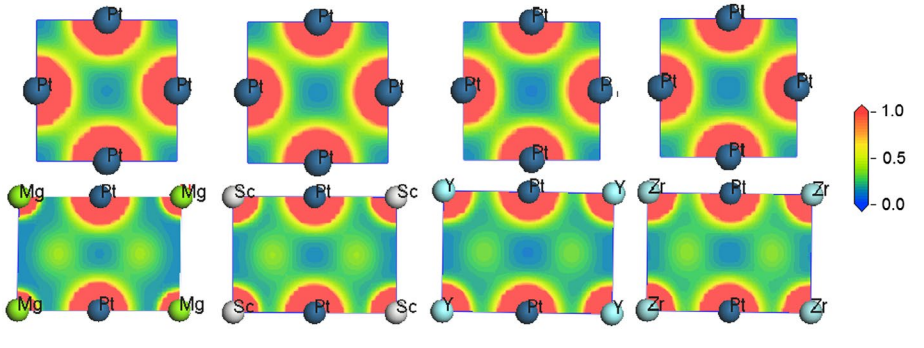

Figure 7. (Colour online) Calculated valence charge density for APt_3 with A=Mg, Ca, Sc, Y and Zr.

Pt-(s,p) states. However, for the APt_3 with A=Sc, Y and Zr, A-d states constitute the hole part of the conduction band, with a small contribution from Pt-d states.

On the other side, different hybridization states are observed in Figure 7. We note the existence of a weak hybridization between Mg-s and Pt-d atoms and a strong one between A-d (A=Sc, Y and Zr) and Pt-d atoms. Our results and conclusions for $ScPt_3$ and YPt_3 consistent with those of Acharya et al.[13].

To give a good comprehension of the bonding in these compounds, we have calculated the overlap population for nearest neighbours in the crystal. Positive values express bonding states between atoms, while negative values are related to antibonding states [39,40]. The present calculations reveal a positive overlapping population between Pt–Pt bonds, then the present bonds are in bonding state. Moreover, high overlap value indicates high degree of covalence in the bond [39,40], all bonds between A–Pt (A=Mg, Sc, Y) atoms are in antibonding state, which return to weaken the stiffness of the crystal, except for $ZrPt_3$ where Zr–Pt bonds are in bonding state. According to the values reported in Table 5, for YPt_3 the Pt–Pt bonds are the strongest. From the calculated atomic population, it can be accessed that Pt atom acquires some electrons from A atoms, which can be explained by the difference in electronegativity of the elements Mg, Sc, Y, Zr and Pt. As a result, ionic bonds will be appear between Pt and A atoms.

To provide a deeper study on the bonding properties, we have calculated the valence charge density in the (0 0 2) and (1 1 0) planes as presented in upper and lower panel, respectively in Figure 7. The electrons are shared between Pt atoms,

Table 5. Bond length and overlap population for nearest neighbours in APt_3 with A=Mg, Sc, Y and Zr.

Comp.	T (K)	P (GPa)	V_{uc} (Å)^3	B (GPa)	α_v (10^{-5} K^{-1})	γ_{th}	C_v (J/mol K)	C_p (J/mol K)	Θ_D (K)
$MgPt_3$	0	0	422.6	211	0.0	2.5	0.0	0.0	324
		50	363	452	0.0	1.9	0.0	0.0	452
	300	0	425.29	210	3.04	2.5	94.35	96.5	319
		50	363.74	445	1.17	1.9	89.36	89.9	450
	1500	0	445	142	5.08	2.9	99.60	121.7	280
		50	369	406	1.45	1.9	99.35	103.6	437
$ScPt_3$	0	0	434.6	237	0.0	2.5	0.0	0.0	341
		50	376	469	0.0	1.9	0.0	0.0	468
	300	0	436.9	228	2.69	2.5	93.75	95.6	336
		50	376.8	463	1.09	1.9	88.66	89.2	466
	1500	0	455	164	4.18	2.8	99.57	117.2	302
		50	382.4	427	1.34	1.9	99.31	103.2	453
YPt_3	0	0	470.3	206	0.0	2.5	0.0	0.0	311
		50	400.6	435	0.0	1.8	0.0	0.0	441
	300	0	473	197	2.92	2.5	94.74	96.9	306
		50	401.3	423	1.10	1.8	89.82	90.3	439
	1500	0	494.7	135	4.74	2.9	99.61	120.2	271
		50	418.3	347	1.54	1.9	99.36	104.0	428
$ZrPt_3$	0	0	449.5	258	0.0	2.4	0.0	0.0	335
		50	391.9	485	0.0	1.8	0.0	0.0	449
	300	0	451.6	249	2.32	2.4	93.94	95.5	331
		50	392.6	479	1.00	1.8	89.47	89.9	448
	1500	0	467	193	3.30	2.6	99.56	112.8	303
		50	397.9	445	1.21	1.9	99.35	102.8	436

it can observed that Pt–Pt bonds are very strong and of covalent nature. A–Pt (A=Mg, Sc, Y and Zr) are less strong and of ionic nature, these results are in agreement with the observed hybridized states in Figure 6.

4. Conclusion

Based on first principle calculations, we have presented a study of structural, elastic and electronic properties of APt_3 with A=Mg, Ca, Sc, Y and Zr. The obtained results are summarised as following:

- The calculated lattice parameters are in good agreement with previous experimental and theoretical data. The APt_3 is more stable when A is a transition metal, this belonging to the presence of d elecrons.
- Elastic constant of single crystal C_{ij} are in satisfactory agreement with the available theoretical data for $ScPt_3$.
- $ZrPt_3$ has the highest bulk, shear, Young modulus and Debye's temperature, So this compound is expected to have the highest melting temperature point among the studied compounds.
- The obtained values of Cauchy's pressure and Poisson's ratio suggest the metallic character of these compounds.
- The calculated values of Pugh's factor show the good malleability of these compounds.
- Elastic constants and their related parameters decrease (increase) when increasing the atomic number in the same column (line) of the periodic table.
- For temperature less than 300 K, bulk modulus B and Debye's temperature Θ_D appear to be independent of temperature, however they (B and Θ_D) decrease slowly with increasing temperature.
- At high temperature, $ZrPt_3$ maintains its highly resistance to volume change against external pressure.
- Volume thermal expansion decreases in the sequence $MgPt_3$, $ScPt_3$, YPt_3 and $ZrPt_3$.
- Thermal Gruneisen parameter γ_{th} decreases by about 25% at high pressure for all compounds under study.
- At normal condition of pressure and temperature (0 GPa, 300 K), calculated thermal constants are slightly affected by the substitution of A elements (A=Mg, Sc, Y and Zr).
- The band structure analysis confirm that these compounds are conductors.
- The bonding mechanism in these compounds, based on the partial densities of states, is based on hybridisation states between A-d and Pt-d atoms.
- From Mulliken analysis of the overlap population, valence charge density and the charge transfer we have confirmed the coexistence of covalent, ionic and metallic bonds in these compounds.

- We conclude that the effect of the size of A atoms and the presence of d electrons could be responsible for the changement in the properties of APt_3 with A=Mg, Ca, Sc, Y and Zr.

Disclosure statement

No potential conflict of interest was reported by the authors.

References

[1] J.K. Stalick and R.M. Waterstrat, *The zirconium–platinum phase diagram*, J. Alloys Compd. 430 (2007), pp. 123–126.

[2] R.E. Schaack, M. Avdeev, W.L. Lee, G. Lawes, H.W. Zandbergen, J.D. Jorgensen, N.P. Ong, A.P. Ramirez, and R.J. Cava, *Formation of transition metal boride and carbide perovskites related to superconducting $MgCNi_3$*, J. Solid State Chem. 177 (2004), pp. 1244–1251.

[3] A. Pandey, C. Mazumdar, and R. Ranganathan, *Magnetic behavior of binary intermetallic compound YPd_3*, J. Alloys compd. 476 (2007), pp. 14–18.

[4] A.O. Pecharsky, Y. Mozharivskyj, K.W. Dennis, K.A. Gschneidner, R.W. McCallum, G.J. Miller, and V.K. Pecharsky, *Preparation, crystal structure, heat capacity, magnetism, and the magnetocaloric effect of $Pr_5Ni_{1.9}Si_3$ and PrNi* Phys. Rev. B 68 (2003), p.134452.

[5] Mark D. Alvey and Patricia M. George, *$ZrPt_3$ as a high-temperature, reflective, oxidation-resistant coating for carbon-carbon composites*, Carbon 29 (1991), pp. 523–530.

[6] S.K. Dhar, S.K. Malik, and R. Vijayaraghavan, *Bor on addition to RPd_3 compounds (R = rare earth)*, Mater. Res. Bull. 16 (1981), pp. 1557–1560.

[7] C. Koenig and D. Knab, *LMTO analysis of the optical conductivity of XPd_3 compounds (X = Sc, Y, La and Ce)*, Solid State Commun. 74 (1990), pp. 11–15.

[8] T. Jeong, *First-principles studies on the electronic structure of $ScPd_3$*, Solid State Commun. 140 (2006), pp. 304–307.

[9] Y. Pan, W.M. Guan, and K.H. Zhang, *First-principles calculation of the phase stability and elastic properties of ZrPt compounds at ground state*, Physica B 427 (2013), pp. 17–21.

[10] K.T. Jacob, K.P. Abraham, and S. Ramachandran, *Gibbs energies of formation of intermetallic phases in the systems Pt-Mg, Pt-Ca, and Pt-Ba and some applications*, Metall. Trans. B 21B (1990), pp. 521–527.

[11] P. J. Meschter and W. L. Worrell, *An investigation of high temperasture thermodynamic properties in Pt-Zr and Pt-Hf systems*, Metall. Trans. A 8 (1977), pp. 503–509.

[12] N. Arikan, A. Iyigör, A. Candan, S. Uğur, Z. Charifi, H. Baaziz, and C. Uğur, *Structural, elastic, electronic and phonon properties of scandium-based compounds ScX_3 (X = Ir, Pd, Pt and Rh): An ab initio study*, Comput. Mater. Sci. 79 (2013), pp. 703–709.

[13] Nikita Acharya, Bushra Fatima, and Sankar P. Sanyal, *Structural and electronic properties of $ScPt_3$ and YPt_3 intermetallic compounds*, J. Metastable Nanocrystall. Mater. 28 (2016), pp. 12–15.

[14] V.I. Razumovski, E.I. Isaev, A.V. Ruban, and P.A. Korzhavyi, *Ab initio calculations of elastic properties of Pt–Sc alloys*, Intermetallics 16 (2008), pp. 982–986.

[15] M.D. Segall, P.J.D. Lindan, M.J. Probert, C.J. Pickard, P.J. Hasnip, S.J. Clark, and M.C. Payne, *First-principles simulation: Ideas, illustrations and the CASTEP code*, J. Phys: Condens. Matter 14 (2002), pp. 2717–2744.

[16] J. Kohanoff, *Electronic Structure Calculations for Solids and Molecules*, Cambridge University Press, Cambridge, 2006.

[17] W. Kohn and L.J. Sham, *Self-consistent equations including exchange and correlation effects*, Phys. Rev. A 140 (1965), pp. 1133–1138.
[18] M.C. Payne, M.P. Teter, D.C. Allan, T.A. Arias, and J.D.J. Joannopoulos, *Iterative minimization techniques for ab initio total-energy calculations: Molecular dynamics and conjugate gradients*, Rev. Mod. Phys. 64 (1992), pp. 1045–1097.
[19] D.M. Ceperley and B.J. Alder, *Ground state of the electron gas by a stochastic method*, Phys. Rev. Lett. 45 (1980), pp. 566–569.
[20] S.J. Clark, M.D. Segall, C.J. Pickard, P.J. Hasnip, M.J. Probert, K. Refson, and M.C. Payne, *First principles methods using CASTEP*, Z. Kristallogr. 220 (2005), pp. 567–570.
[21] B.G. Pfrommer, M. Cote, S.G. Louie, and M.L. Cohen, *Relaxation of crystals with the Quasi-Newton method*, J. Comput. Phys. 131 (1997), pp. 133–140.
[22] H.J. Monkhorst and J.D. Pack, *Special points for Brillouin-zone integrations*, Phys. Rev. B 13 (1976), pp. 5188–5192.
[23] R. Fouret, B. Hennion, J. Gonzalez, and S.M. Wasim, *Elastic stiffness constants of copper indium diselenide determined by neutron scattering*, Phys. Rev. B 47 (1993), pp. 8269–8272.
[24] F. Birch, *Finite elastic strain of cubic crystals*, Phys. Rev. 71 (1974), pp. 809–824.
[25] V. Milman and M.C. Warren, *Elastic properties of TiB_2 and MgB_2*, J. Phys. 13 (2001), pp. 5585–5595.
[26] E. Schreiber, O.L. Anderson, and N. Soga, *Elastic Constants and Their Measurement*, McGraw-Hill, New York, NY, 1973.
[27] J. Wang, S. Yip, S.R. Phillpot, and D. Wolf, *Crystal instabilities at finite strain*, Phys. Rev. Lett. 71 (1993), pp. 4182–4185.
[28] M.L. Cohen, *Calculation of bulk moduli of diamond and zincblende solids*, Phys. Rev. B 32 (1985), pp. 7988–7991.
[29] V.V. Bannikov, I.R. Shein, and A.L. Ivanovskii, *Elastic properties of antiperovskite-type Ni-rich nitrides $MNNi_3$ (M=Zn, Cd, Mg, Al, Ga, In, Sn, Sb, Pd, Cu, Ag and Pt) as predicted from first-principles calculations*, Physica B 405 (2010), pp. 4615–4619.
[30] Efthimios Kaxiras, *Atomic and Electronic Structure of Solids*, Cambridge University Press, New York, NY, 2003.
[31] J. Haines, J.M. Léger, and G. Bocquillon, *Synthesis and design of superhard materials*, Annu. Rev. Mater. Res. 31 (2001), pp. 1–23.
[32] S.F. Pugh, *Relations between the elastic moduli and the plastic properties of polycrystalline pure metals*, Philos. Mag. 45 (1954), pp. 823–843.
[33] J.P. Poirier, *Introduction to the Physics of the Earth's interior*, 2nd ed., Cambridge University Press, Cambridge, 2000.
[34] M.A. Blanco, A. Martin Pendas, E. Francisco, J.M. Recio, and R. Franco, *Thermodynamical properties of solids from microscopic theory: Applications to MgF_2 and Al_2O_3*, J. Mol. Struct. Theochem. 368 (1996), pp. 245–255.
[35] M.A. Blanco, E. Francisco, and V. Luaña, *GIBBS: isothermal-isobaric thermodynamics of solids from energy curves using a quasi-harmonic Debye model*, Comp. Phys. Commun. 158 (2004), pp. 57–72.
[36] J.J. Gilman, *Electronic Basis of the Strength of Materials*, Cambridge University Press, Cambridge, 2003.
[37] Z. Sun, D. Music, R. Ahuja, and J.M. Schneider, *Ab initio of M_2AlN (M = Ti, V, Cr)*, J. Phys. Condens. Matter 17 (2005), p. L15–L19.
[38] G. Hug, *Electronic structures of and composition gaps among the ternary carbides Ti_2MC*, Phys. Rev. B 74 (2006), p. 184113.
[39] M.D. Segall, R. Shah, C.J. Pickard, and M.C. Payne, *Population analysis of plane-wave electronic structure calculations of bulk materials*, Phys. Rev. B 54 (1996), pp. 16317–16320.
[40] M.D. Segall, *Population analysis in plane wave electronic structure calculations*, Mol. Phys. 89 (1996), pp. 571–575.